Figures with Legends

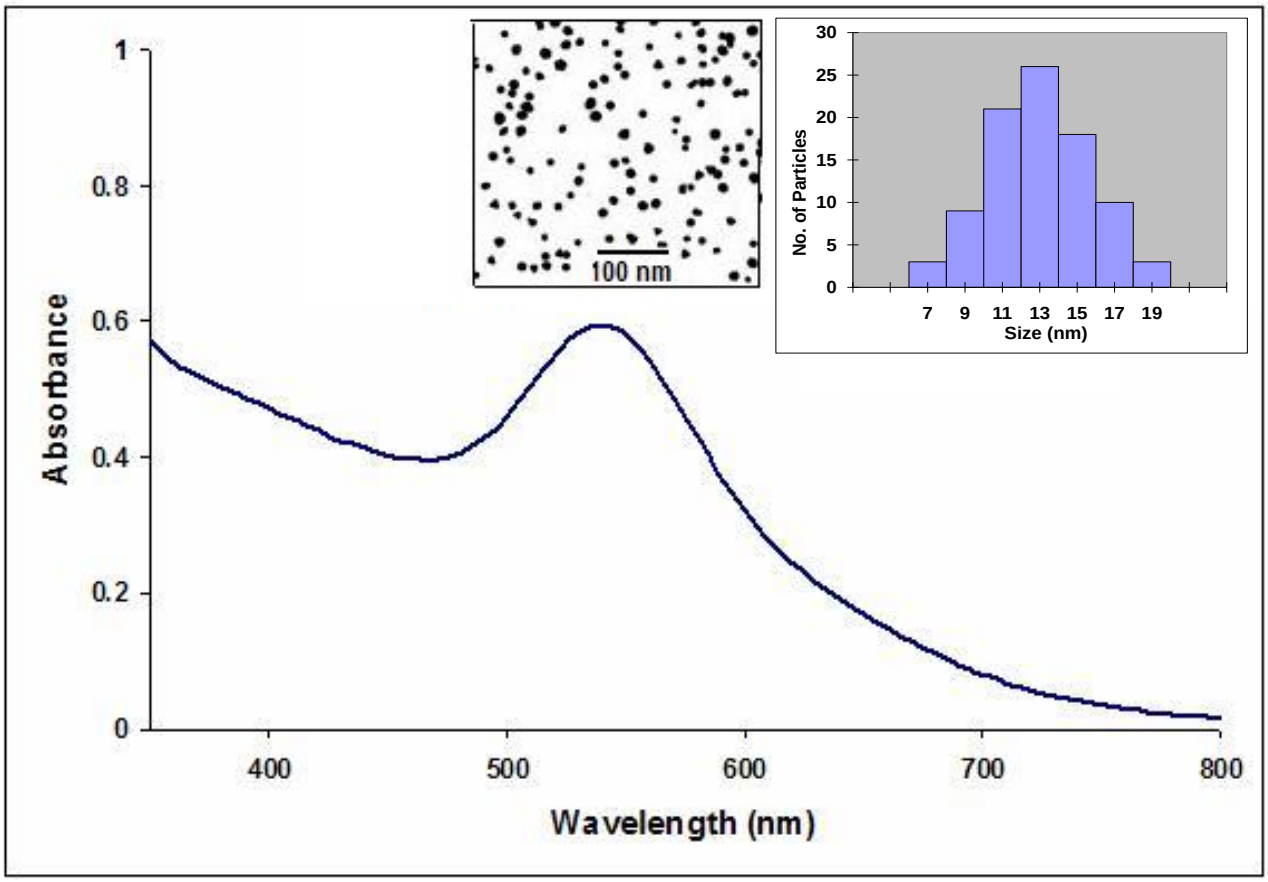

Fig. 1. UV-visible spectrum of Cin-AuNPs synthesized using cinnamon. The inset shows the TEM and size distribution histogram of the gold nanoparticle solution formed at the end of the reaction.

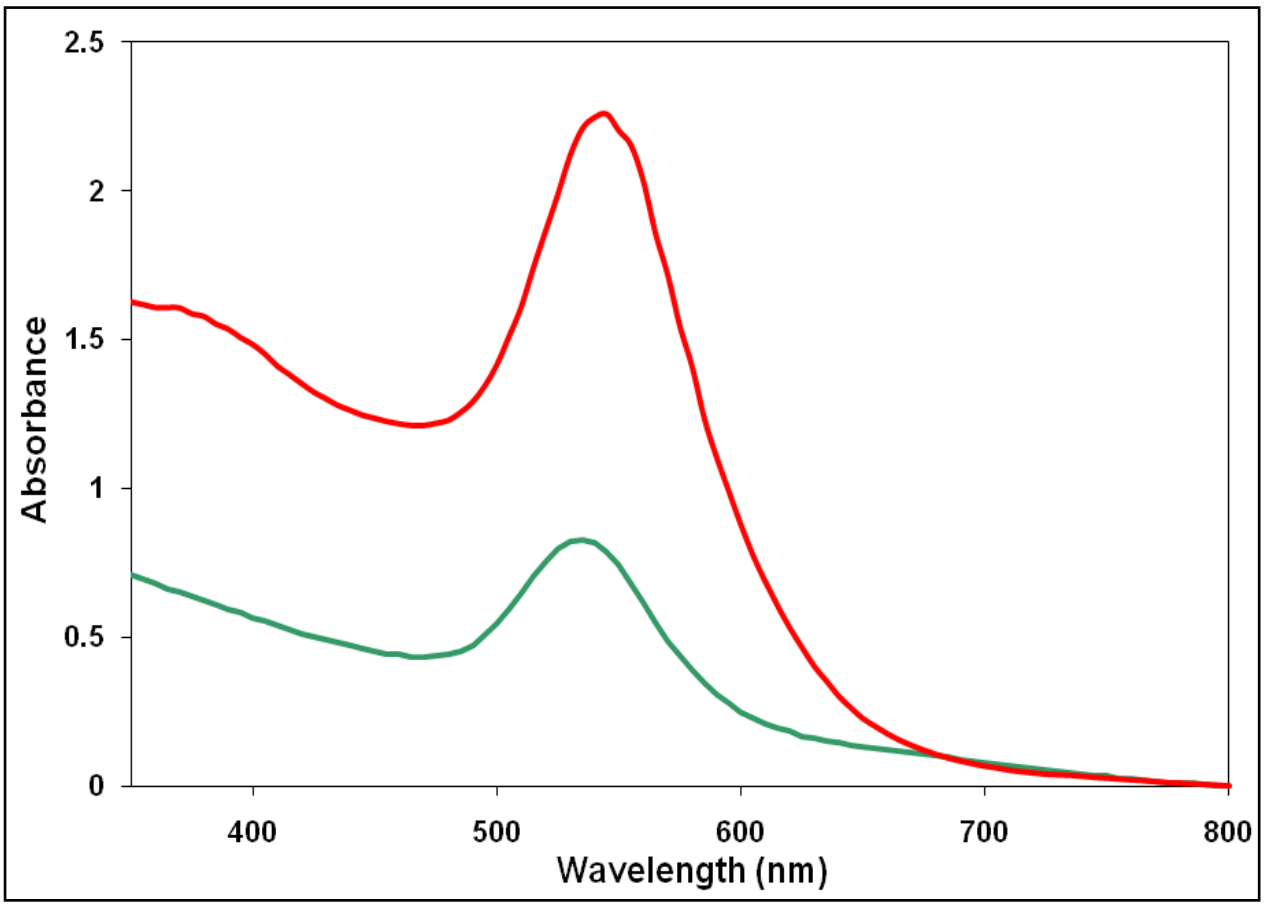

Fig. 2. Synthesis of gold nanoparticles using cinnamon phytochemicals, cinnamaldehyde (red) and linalool (green).

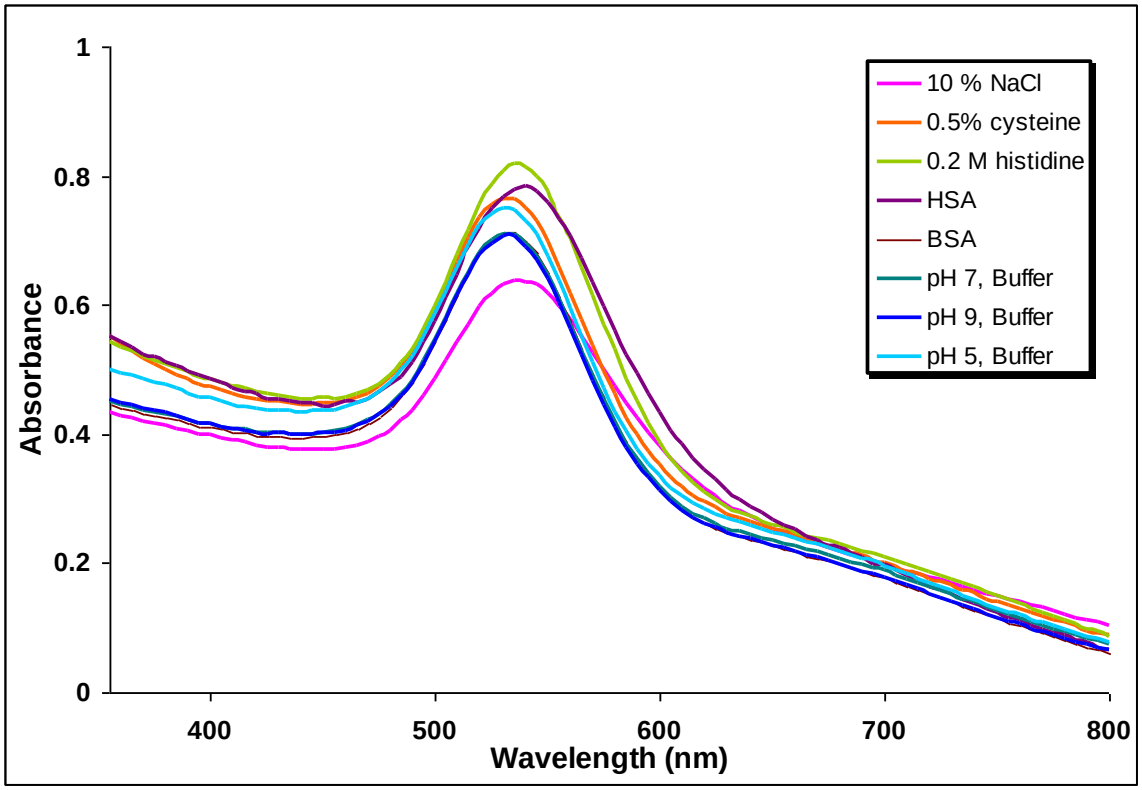

Fig. 3. UV-visible spectra of Cin-AuNPs showing *in vitro* stability of the nanoparticles in different medium, e.g., 10 % NaCl, 0.5 % cysteine, 0.2M Histidine, 0.5 % HSA, 0.5 % BSA and in different pH after 24 hours treatment.

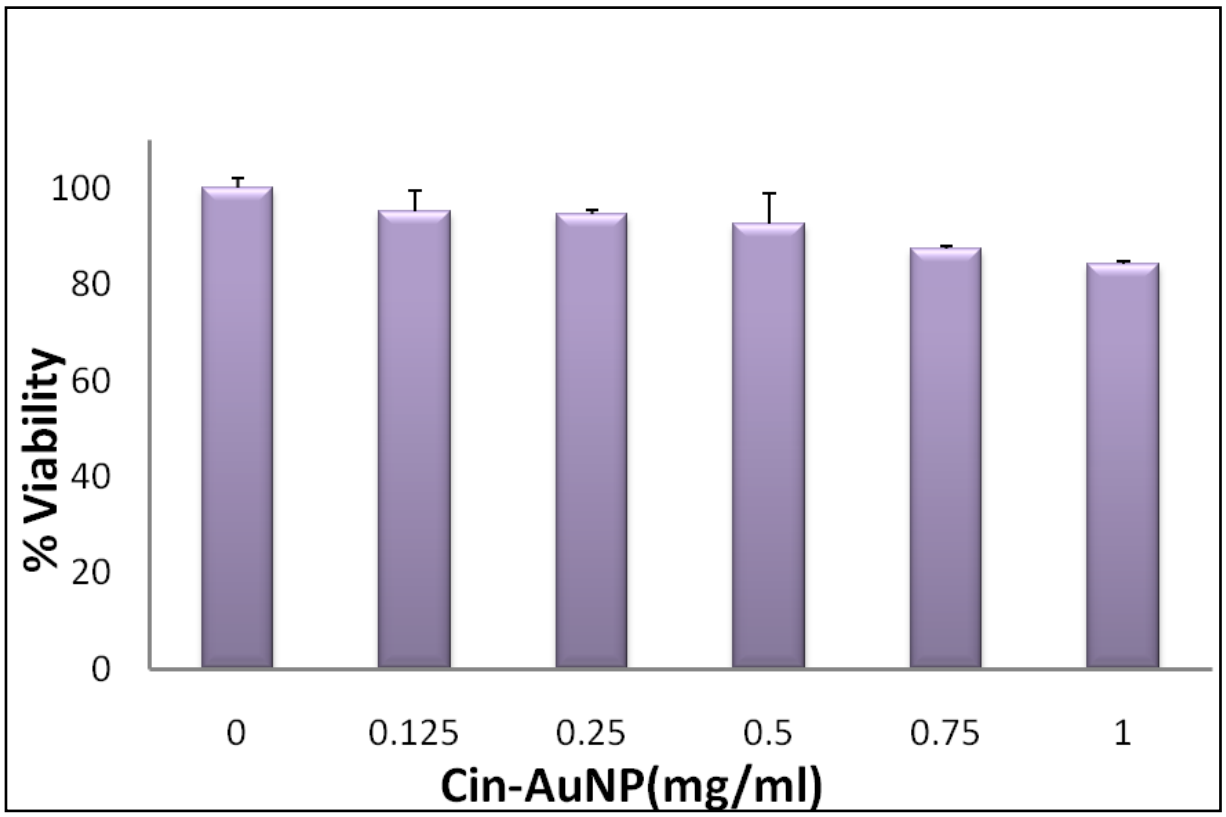

Fig. 4. Cell viability of fibroblast cells after 24 hours of incubation with increasing amounts of Cin-AuNPs showing non toxic profiles.

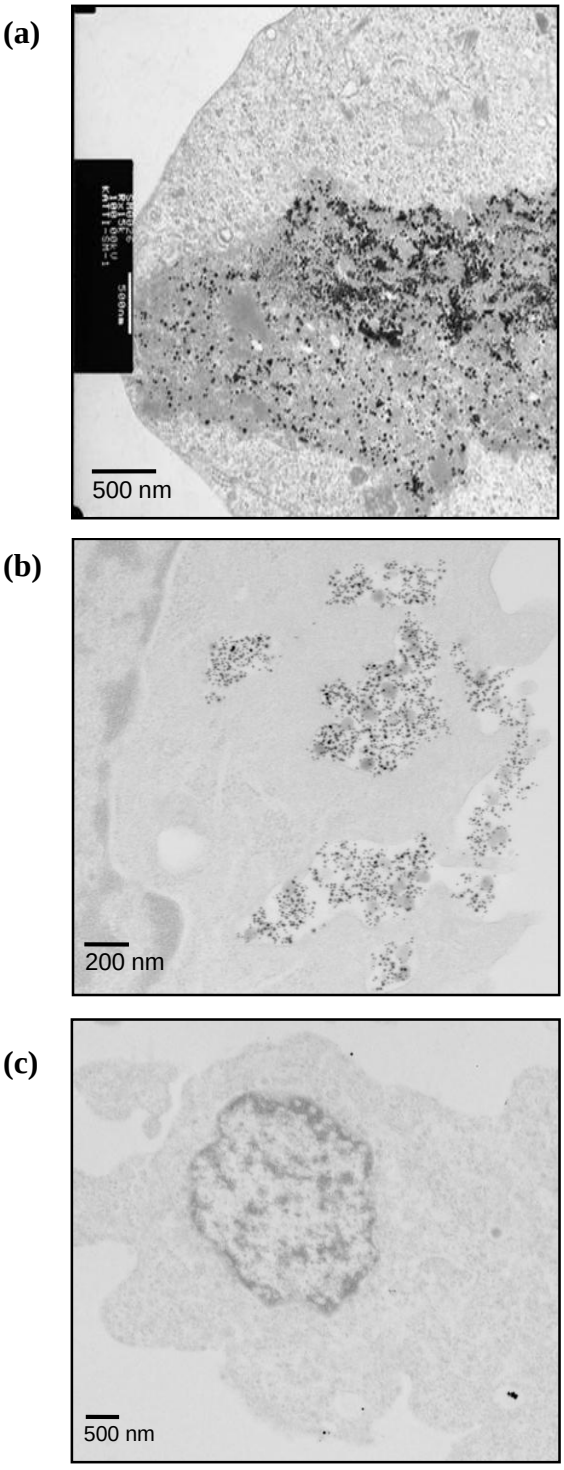

Fig. 5. TEM images showing (a) MCF-7, (b) PC-3 cells internalizations of Cin-AuNPs and (c) PC-3 cells internalization of Cinnamaldehyde-AuNPs. The concentration of Cin-AuNPs, internalized within PC-3 and MCF-7cells, is an order of magnitude higher than the concentration of Cinnamaldehyde-AuNPs in PC-3 cells.

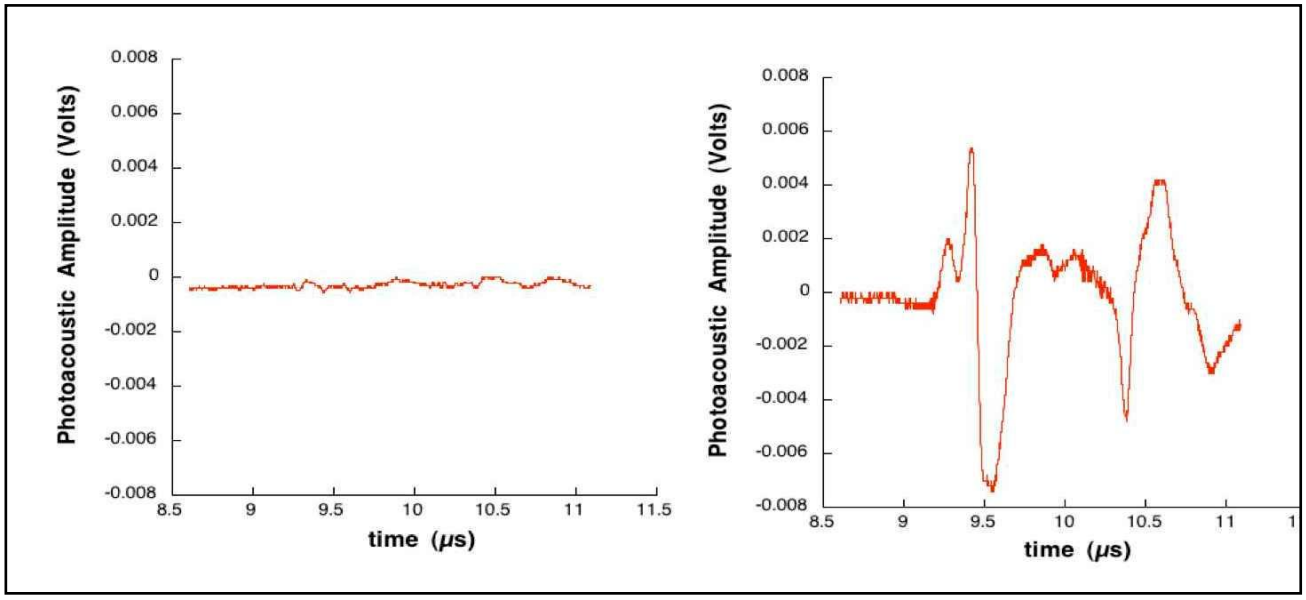

Fig. 6. Detection of photoacoustic signals by irradiating Cin-AuNPs tagged prostate cancer cells. Irradiating only PC-3 cells gives no signals (Left) whereas irradiating Cin-AuNPs tagged 15 prostate cancer cells under flow show strong photoacoustic signals (Right).

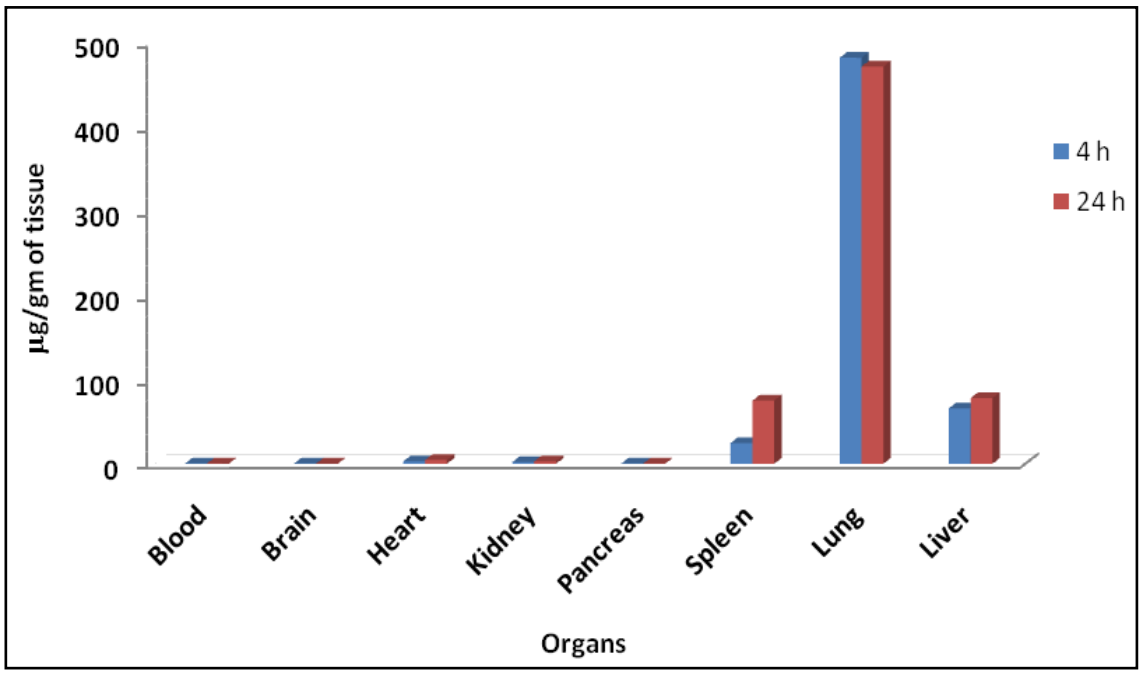

Fig. 7. Biodistribution of Cin-AuNPs in mice model. The concentration of gold in various organs was analyzed by AAS.

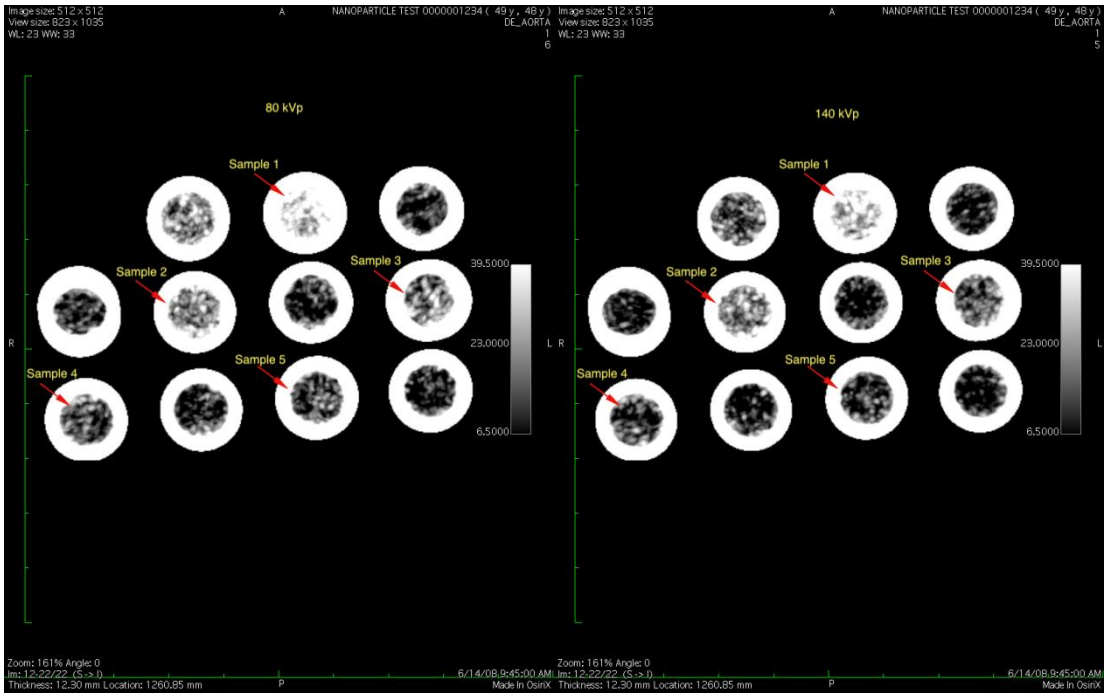

Fig. 8. Maximum intensity projection (MIP) CT images of the samples at (a) 80 and (b) 140 kVp. Vials containing Cin-AuNP with the concentrations of 880 (Sample 1), 704 (Sample 2), 528 (Sample 3), 352 (Sample 4), and 176 (Sample 5) µg/mL.

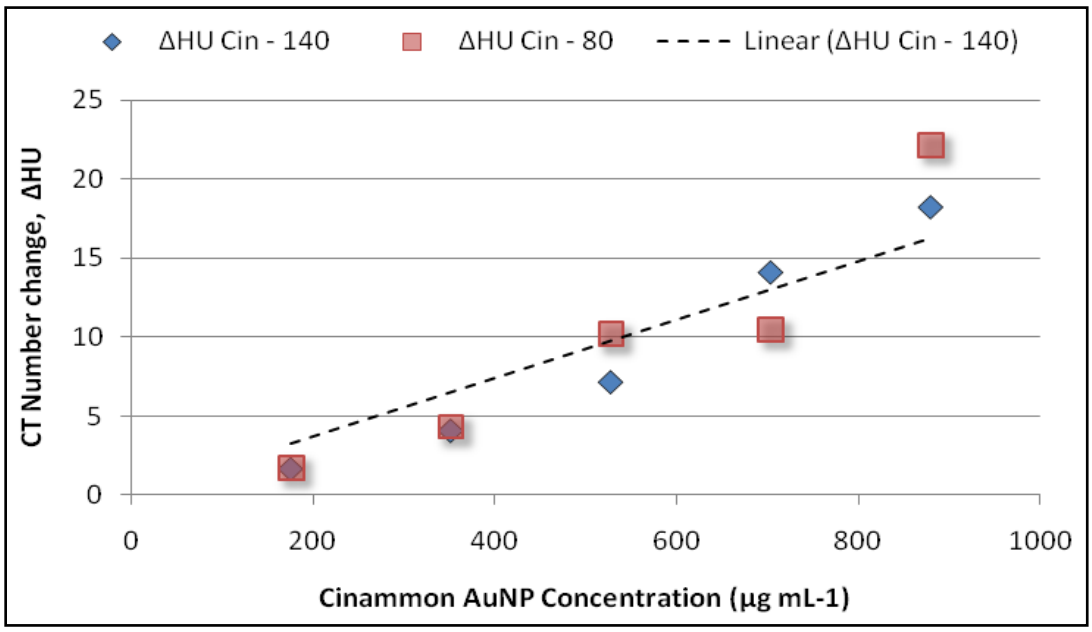

Fig. 9. Linear dependence of ΔHU on the increasing concentration of Cin-AuNPs in CT experiments. Sample concentrations range from 176 µg mL^{-1} to 880 µg mL^{-1}. The line represents a linear fit throught the 140 kVp data. The slope of this line is y = 0.0185•x.